Ultrasound Calibration Toolkit with a High-Adjustability Feature Based on User Requirements

Maria Chatrasingh[1,2], Jackrit Suthakorn, Ph.D.[1,2,*], Songpol Ongwattanakul, Ph.D.[1,3], Cholatip Wiratkapun, M.D.[4], Somkiat Huaijantug, Ph.D.[5]
[1]Center for Biomedical and Robotics Technology, [2]Dept of Biomedical Engineering, [3]Dept of Computer Engineering, Faculty of Engineering,
[4]Department of Radiology, Faculty of Medicine Ramathibodi Hospital, [5]Faculty of Veterinary Science, Mahidol University, Thailand. *Corresponding Author: egjst@mahidol.ac.th

***Abstract*—3D freehand Ultrasound reconstruction is one of the techniques to assemble 3D ultrasound volume from 2D ultrasound images. Its benefits include low-cost operations, conveniency and ease of usage which can be applied to intra-operative imaging. Ultrasound calibration is the procedure needed to be performed on a 2D ultrasound machine before turning it into 3D freehand ultrasound. This procedure is used to find the position and orientation of each acquired 2D ultrasound image in 3D space while freely moving the ultrasound probe to collect images and reconstruct them on 3D volume. In this paper, we propose our ultrasound calibration system, programmed to be an automated calibration tool—the efficient, convenient and suitable for regular ultrasound calibration performance. The system provides user interface for collecting data from calibration performance, automatic ultrasound image segmentation and calibration in an orderly manner. The users are not required to manually select the proper image set or extract images' feature as an input for the system as opposed to other regular procedures. An option to switch to semi-automated mode is also added to overcome the problem of segmenting the input images which are low in quality. Hopkins phantom and N-based phantom are supported by the prototype system for the sake of further development.**

Keywords-Ultrasound; Calibration; Freehand; Phantom; Feature extraction; Hopkins; N-based;

1. Introduction

Ultrasound imaging or ultrasonography is a fast, non-invasive and inexpensive medical imaging modality. Due to its property of real-time image acquisition, it is sometime used in the guidance of intervention procedures such as in tissue biopsy or intra-operative monitoring. However, the fast, non-invasive and inexpensive nature can only be found in 2D ultrasound imaging. The lack of 3D information and its reference point to the physical world are the tradeoffs to this effectiveness.

3D freehand ultrasound reconstruction is one of many options to acquired 3D ultrasound volume. This technique reconstructs sets of tracked 2D ultrasound images to their tracked positions and orientation. However, to produce a reference point in that 3D volume, the calibration of ultrasound probe is necessary before the intervention.

Ultrasound probe calibration is a procedure used to find rigid transformation from the ultrasound image coordinate to the ultrasound probe coordinate, or to accurately align each ultrasound image onto a physical coordinate. This procedure is performed by rigidly fixed a position and orientation sensor of the tracking system to the ultrasound probe. The sensor, working with the tracking system, gives an account of tracking the probe's position and orientation in real time according to a reference point. The probe is then used to scan the 3D phantom with known geometry from many viewpoints. After acquiring enough images, pixel locations in each image which characterize the phantom are registered to their own 3D geometries to find the mathematical relations of the ultrasound image coordinate and the ultrasound probe coordinate.

Most research in ultrasound calibration is now focusing on developments of calibration phantom designs extending from traditional designs [1, 2] to more and more modern designs; for instance, 2D alignment phantom [3-5], Hopkins phantom [6], N-based phantom [7-9], and pointer-based phantom [10, 11]. These modern designs gain more benefit of automation in their images' feature extraction. Many automated algorithms are proposed to support the modern designs but none offers the ability to classify whether an input ultrasound image provides sufficient features inside; the algorithms assume that every frame of collected image contains adequate features leading to incorrect extraction. Prager *et al.* once suggested the moving of an ultrasound probe to cover all the necessary degrees of freedoms to avoid solution degeneracy [12]. Nevertheless, moving the probe freely in all degree might cause some acquired images to lose the feature. The selection of image frames from hundreds of collected ultrasound images are yet the burdens posted upon the calibrated operators before enter the automated part.

In this paper, an intelligent automated ultrasound calibration system has been developed with an ability to classify images: whether within them exists phantom's features and automatically segment that feature from the image. The user no longer manually finishes this task as conventional ways.

The system selects images with sufficient feature first before searching in detail, thus, reduce the computational load. Although this system can operate itself automatically, the high adjustability feature of the system offers the user to stop the automation and participate in the semi-automation.

More adjustability features include the supported designs of the phantoms. Two important ultrasound

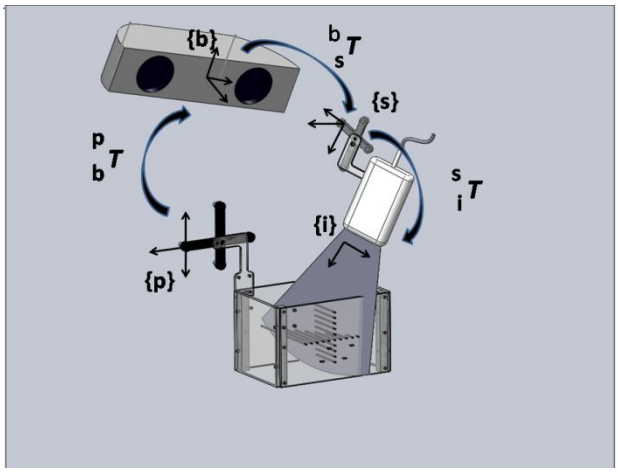

Fig. 1. Diagram of ultrasound calibration procedure.

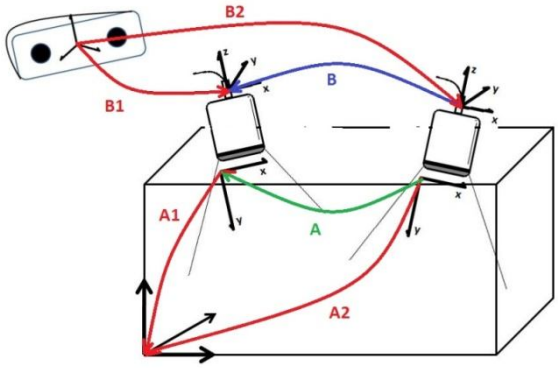

Fig. 2. Diagram of Hand-Eye transformation.

calibration phantoms; Hopkins phantom and N-based phantom, are supported without restriction on each design's variation. The varieties in each design, such as, scale of the constructed pattern or number of pattern replication, are acceptable. The algorithm chosen to establish the system is tolerance to speckle noise from ultrasound. Therefore, the variation of ultrasound probe's specifications (linear array or convex array transducer) can be calibrated with our proposed system.

2. Background

Mathametical Background

As mentioned in the introduction, the setting of the ultrasound calibration procedure consists of position tracking system, an ultrasound machine with its probe, and the phantom with known geometry as shown in Fig.1. The tracked ultrasound calibration phantom is scanned with the tracked ultrasound probe from various directions. The series of ultrasound images are collected along with the corresponding transformation matrix from the position sensor attached to the probe to the base unit of the tracking system ${}^{b}_{s}T$ and the transformation matrix from the base unit to tracked phantom ${}^{p}_{b}T$. ${}^{s}_{i}T$ is the constant transformation matrix from 2D ultrasound image to the position of the sensor attached to the probe which we attempt to find from ultrasound probe calibration. The equation to register image coordinate to the phantom coordinate is set as the following:

$$\begin{bmatrix} X_c \\ Y_c \\ Z_c \\ 1 \end{bmatrix} = {}^{p}_{b}T \; {}^{b}_{s}T \; {}^{s}_{i}T \begin{bmatrix} s_x u \\ s_y v \\ 0 \\ 1 \end{bmatrix} \quad (1)$$

With the known geometry of phantom, the mapping of image's coordinate $[u\ v]^T$ to corresponding phantom's geometry $[X_c\ Y_c\ Z_c]^T$ is defined. ${}^{b}_{s}T$ is reported from tracking system, ${}^{p}_{b}T$ is known from the phantom's geometry, leaving only ${}^{s}_{i}T$ to be identified. The matrix consists of 6 variables; 3 rotation angles and 3 translations, when combine with two scale factors; s_x and s_y, there are total of 8 unknown parameters to be determined.

The iterative method of Levenberg-Marquardt non-linear least squares optimization is used to define all eight variables. This method has been shown to offer accurate results for calibration [6].

A good initialization is required for the optimization algorithm to easily reach the true parameter values. Closed form solution of hand-eye transformation has been reported to generate the promised solution on ultrasound probe calibration [7, 13]. We use this closed form solution to determine the initial parameters for N-based phantom. Equation (2) is hand-eye transformation equation;

$$AX = XB \quad (2)$$

According to Fig. 2 and Eq. (2), A is the transformation matrix between two images' coordinate systems. A can be acquired from $A = A_2 A_1^{-1}$ while B is the transformation between two position sensor coordinate system corresponding to the images. B is acquired from $B = B_2^{-1} B_1$. X is a transformation matrix from images' coordinate to probe's position sensor coordinate. This transformation is the unknown matrix needed to be defined. X transformation matrix can be found from closed form solution

$$\begin{bmatrix} I_9 - R_a \otimes R_b & 0_{9*3} & 0_{9*3} \\ I_3 \otimes t_b^t & I_3 - R_a & -D_u \end{bmatrix} \begin{bmatrix} vec(R_x) \\ t_x \\ \lambda_{3*1} \end{bmatrix} = \begin{bmatrix} 0_{9*1} \\ 0_{3*1} \end{bmatrix} \quad (3)$$

R_a, R_b, and R_x are rotation matrices extracted from A, B and X matrix respectively so as t_b and t_x the translation vectors from corresponding matrices. The vec and $\otimes$ are operator vec and Kronecker product respectively.

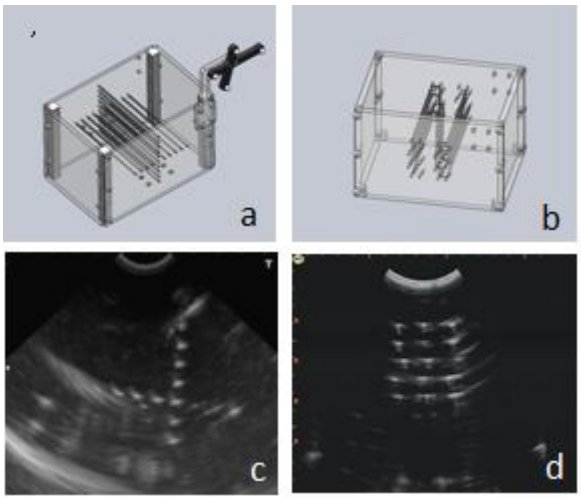

Fig. 3. Phantom designs and corresponding ultrasound images. (a) and (c) are Hopkins phantom's design and ultrasound image from scanning this design respectively while (b) and (c) are from N-based phantom.

Phantom's Designs Background

Our system supports two designs of calibration phantom. The two designs are claimed to return ultrasound images with ability to be automatically segmented. Since both phantoms produce its feature in ultrasound images as dots with special characteristic of alignments, almost same algorithm for segmentation can be applied. In the field of ultrasound calibration, the designs of Hopkins and N-based are famous templates for other extensive designs [14, 15]. In addition, a lot of research has proposed new algorithms to supports these designs [9, 14, 16].

- Hopkins phantom design

The Hopkins phantom's structure consists of two parallel plastic plates. Stretched between them are several parallel nylon lines in the pattern to form two orthogonal planes. The design is shown in Fig. 3(a) with the corresponding ultrasound image in Fig. 3(c). One translational parameter along the nylon lines axes is unidentified thus two from total of three equations per one point can be discriminated from Eq. (1).

- N-based phantom design

N-based phantom is constructed with two plastic plates stretched with nylon lines in pattern to form multiple N-shapes aligned in parallel planes as shown in Fig. 3(b). The ultrasound image result of scanning this phantom is also shown in Fig. 3(d).

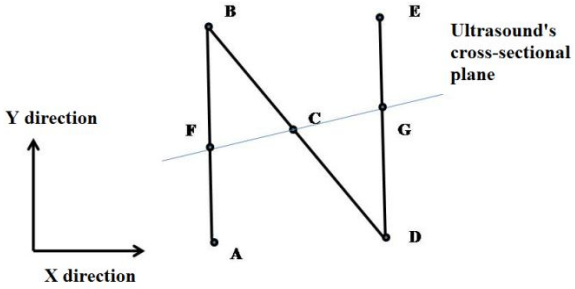

The equation used with this design of phantom is shown in Eq. (1) where X_c, Y_c and Z_c can be estimated by Eq. (4) and Eq. (5) according to Fig. 4.

Fig. 4. The geometry of N-shape provides the position where the phantom crosses the ultrasound plane.

$$X_C = X_B + \left(\frac{CF}{FG}\right)(X_D - X_B) \quad (4)$$

$$Y_C = Y_B + \left(\frac{CF}{FG}\right)(Y_D - Y_B) \quad (5)$$

Z_c depends on the construction of the phantom and to which of N shapes those points belong. *Xc*, *Yc* and *Zc* are placed in Eq. (1).

From Eq. (1), all eight parameters are identified with initialization of parameters and optimizing the values with Levenberg-Marquardt nonlinear implementation.

3. Methodology

This system is programmed in MATLAB®. It consists of convenient graphical user interface for ease of use and conveniency. Under the interface window is an automatic calibration algorithm which will be terminated and return calibration results when the calibration parameters cause acceptable error.

The system is created with the strong intention to make the calibration procedure become simpler. Therefore, the process after data collecting is fully automated. However, the user is able to stop the automation, and interact on image segmentation process in case of poor segmentation results return.

The system can be separated into two parts. First, the part of automatic image feature extraction. The second is the part of the parameters optimization.

A. Automatic Image Feature Extraction

The algorithm for image feature extraction is capable of extracting the feature for Hopkins phantom and N-based phantom designs. Therefore the description given below is relevant for both of the designs. The system feeds the algorithm image by image. Each input image's boundary area is cropped to excluding the image' label. The threshold setting by half of the image's maximal intensity decreasing the number of region to be focused on (around twenty regions in each image). These remaining regions are shrunken to their own weight-centroid points. All these

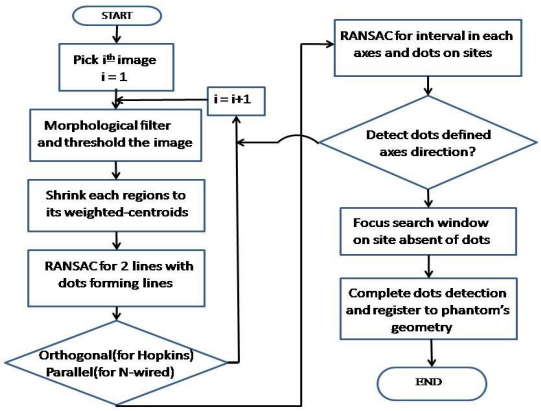

Fig. 5. Flowchart for image feature extraction

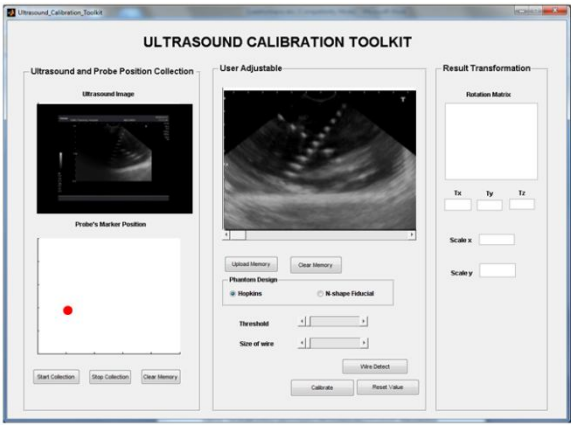

Fig. 6. Graphic User Interface (GUI) of our ultrasound calibration toolkit.

centroids are then sent to Random Sample Consensus algorithm.

Random Sample Consensus (RANSAC) algorithm is a robust iterative method for estimation parameters of mathematical models from data. RANSAC algorithm is employed twice in our image feature extraction algorithm.

The first employment is used to determinate parameters of a line resulted from dots alignment in the image. The algorithm works by randomly select the group of dots until it finally finds the group which give the excellent characterize of lines. The possibility score given for each group is based on distance errors from the line to every dot in the group. The lines mentioned are the two orthogonal lines in Hopkins phantom's images, and the multiple lines are about parallel from N-based phantom. The logic gate with the condition of orthogonality or parallelism is used as the pre-classifier whether an ultrasound image contain sufficient details inside.

In the second employment, RANSAC algorithm is used to estimate a constant distance gaps between dots or lines.

The RANSAC algorithm always returns a list of data possibly conformed to the mathematical models. This data is called inlier. The data which is not in the manner of others is called outlier data. It is excluded from the parameter estimation. Therefore, this algorithm is perfectly fit to ultrasound image of which noises are classified as speckle noises (usually present with granular white dots randomly distributed). This characteristic of noise can be misclassified as dots in the feature pattern.

Sequence of image segmentation procedure is presented as a flowchart in Fig. 5.

B. Automatic Calibration

Calibration of the system uses Levenberg-Marquardt optimization algorithm for both Hopkins and N-based phantoms. Initialization of parameters is as follow. For Hopkins phantom, the ultrasound plane alignment has to cross with both planes of nylon lines. If the image's plane paralleled or almost paralleled to one of the two phantom planes, it would not cross with nylons on the other plane which leading to insufficient features contain in the image. As a result, we use the ultrasound plane which coincides with coronal plane of the phantom for calculation of parameters' initialization.

Three rotational parameters and two translational parameters (translation along nylons' axis is excluded) of image's plane to ultrasound probe is estimated by the method as follow. The ultrasound image which present with minimal gap distance between dots is chosen. The minimal distance implies this image to be caption of near coronal cross-section plane of the phantom; the coronal plane makes the nearest gap distance. We assume its corresponding geometries on the phantom's coronal plane. Horn's method of plane-to-plane transformation [17] is used to estimate the transformation matrix from features in this image to its phantom's geometry; ${}^{p}_{i}T$. Therefore, ${}^{s}_{i}T$ is calculated back by

$$ {}^{s}_{i}T = {}^{b}_{s}T^{-1}\,{}^{p}_{b}T^{-1}\,{}^{p}_{i}T \tag{6} $$

with ${}^{b}_{s}T$ and ${}^{p}_{b}T$ acquired from tracking data.

This ${}^{s}_{i}T$ is then conversed to five initial parameters of the optimization problem.

Two scale factors are later extracted by solving the least square linear equations from initial ${}^{p}_{i}R$; the component of initial ${}^{p}_{i}T$.

$$ \begin{bmatrix} X_c \\ Y_c \\ Z_c \end{bmatrix} = \begin{bmatrix} R_{11} & R_{12} & R_{13} \\ R_{21} & R_{22} & R_{23} \\ R_{31} & R_{32} & R_{33} \end{bmatrix} \begin{bmatrix} s_x u \\ s_y v \\ 0 \end{bmatrix} + \begin{bmatrix} t_x \\ t_y \\ t_z \end{bmatrix} \tag{7} $$

R_{ij} is an element of ${}^{p}_{i}R$. t_x, t_y and t_z are the elements of translation vector estimated using initial ${}^{p}_{i}T$.

From Eq. (7), we have

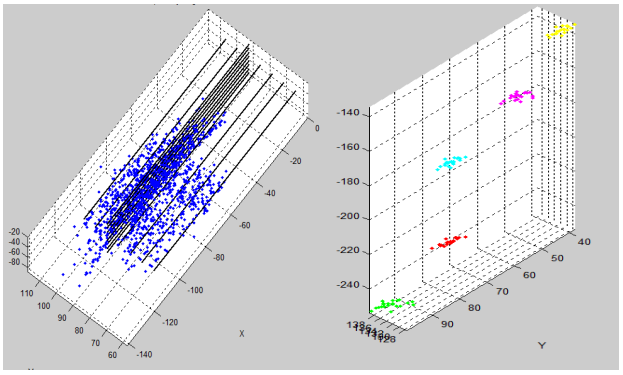

Fig. 7. 3D back reconstruction of Hopkins (Left) and N-based (Right) phantoms.

$$\begin{bmatrix} X_c - t_x \\ Y_c - t_y \\ Z_c - t_z \end{bmatrix} = \begin{bmatrix} uR_{11} & vR_{12} \\ uR_{21} & vR_{22} \\ uR_{31} & vR_{32} \end{bmatrix} \begin{bmatrix} s_x \\ s_y \end{bmatrix} \quad (8)$$

and using $[s_x \quad s_y]^T$ as the initial values for two scale factors.

For N-based phantom, ${}^{s}T_i$ and two scale factors can be initialized from closed form solution of hand-eye transformation; Eq. (3).

C. The Graphical User Interface

The main goal to design the graphical user interface is to introduce an easy-to-use and less complicated mean for the users who may not be familiar with the knowledge behind calibration procedure. The user interface window is divided into 3 parts as seen in Fig. 6; the data collection part, semi-automated image segmentation part and results return part.

The data collection part is the part that connects to the tracking device and the ultrasound capture device to receive both corresponding data in sequencing. The collecting part input is the continuing data and the system, by itself, is able to classify the raw sequence of ultrasound images and select only the images which contain enough feature of the phantom.

The semi-automated image segmentation part is the part in which the user can be involved in image segmentation task; modify the threshold level or the diameter of nylons' feature, in case the input ultrasound images are low in quality. However, in the ultrasound images with lesser noise interference, the user can skip this part and continue with automated segmentation provided.

The third part is the part which returns the results of calibration consisting of a rotation matrix, a translation vector and two scale factors as described in the background.

4. Result and Discussion

Our ultrasound calibration system provides the tool to suit the regular calibration performance. The tool is created to be automated for convenience in calibration procedures where regular procedures require longer time period and more background knowledge to operate. In order to make our system automated, we propose new automatic image feature extraction for two phantom's designs. We also propose the new algorithm of automatic parameter initialization in Hopkins phantom.

After having tested the system on a personal computer with Intel® Core™2 Duo Processor 2.2 GHz, 2GB DDR RAM and NDI POLARIS VICRA optical tracking system for the ultrasound calibration procedure, the collection of corresponding two data types took about 1 second per frame. For automatic image segmentation, the time taken in detecting and registering all dots in each image acquired from Hopkins phantom was approximately 0.6 second and 0.4 second for N-based phantom respectively. The miss-detect rate are 7.5% of sufficient-feature image in Hopkins phantom and 4.3% for N-based phantom. The time for calibration part varied depending on the characteristic and the amount of acquired images easily reaching the optimum value. Figure 7 shows that after being optimized with data from our automated algorithm for feature detection and initialized with our automatic parameter initialization, the resulting calibration parameters could reconstruct the data back to each phantom's geometry.

We also tested another deviation on our Hopkins phantom's initialization method. The two scale factors were estimated from the same least square method but using optimized ${}^{p}_{i}R$ instead of the initial one. The acquire scale factors are almost the same as those from the first method without sending these two parameters into optimization process.

5. Conclusion

Our ultrasound calibration system is capable of defining transformation matrix derived from imagery space and probe's coordinates with robust algorithm in extracting image's features while retaining the capability of automation. Furthermore, we aim to extend the system to support all main designs of calibration phantoms and evaluated results' error as well as reproducibility compared to the non-automated systems. For our main objective, this calibration toolkit will be included as a component in our freehand ultrasound system. We also hope that our calibration system be widely used in the field of researches; either in freehand ultrasound system or other applications, and in practical procedure in the future.

Acknowledgement

Small Animal Hospital, Faculty of Veterinary Science, Mahidol University, Thailand for supporting all ultrasound equipments on our research. This project is supported by the Royal Thai Government through Mahidol University. The first author is supported by the Mahidol University Ph.D.-M.D. program.

References

[1] R.W. Prager, R.N. Rohling, A.H. Gee, L. Berman, "Rapid calibration for 3-D freehand ultrasound" *Ultrasound Med and Biol.*, vol. 24, no.6, pp. 855-869, 1998.

[2] P. R. Detmer, G. Bashein, T. Hodges, K. W. Beach, E.P. Filer, D. H. Burns, , and D. S. Jr., "3d ultrasonic image feature localization based on magnetic scanhead tracking: in vitro calibration and validation," Ultrasound in Medicine and Biology 20(9), pp. 923–936, 1994.

[3] D.F. Leotta, "An effcient calibration method for freehand 3-D ultrasound imaging systems," Ultrasound in Medicine & Biology, 30, 999–1008.

[4] F. Lindseth, J. Bang , T. Langø, "A robust and automatic method for evaluating accuracy in 3-D ultrasound-based navigation," Ultrasound in Medicine & Biology, 29, 1439–1452.

[5] J.N. Welch, J.A. Johnson, M.R. Bax, R. Badr, R. Shahidi, "A real-time freehand 3D ultrasound system for image-guided surgery," IEEE Ultrasonics Symposium, vol. 2, 1601–1604.

[6] E.M. Boctor, A. Jain, M.A. Choti, R.H. Taylor, G. Fichtinger, "A rapid calibration method for registration and 3D tracking of ultrasound images using spatial localizer," Proceedings of SPIE, vol. 5035, 2003, pp. 521-532.

[7] E. Boctor, A. Viswanathan, M. Choti,, R.H. Taylor, G. Fichtinger, G. Hager, "A novel closed form solution for ultrasound calibration," IEEE International Symposium on Biomedical Imaging, vol. 1, 2004, pp. 527-530.

[8] N. Pagoulatos, D.R. Haynor, Y. Kim, "A fast calibration method for 3-D tracking of ultrasound images using a spatial localizer," Ultrasound in Medicine & Biology, 27, 1219–1229.

[9] T.K. Chen, P. Abolmaesumi, A.D. Thurston, R.E. Ellis, "Automated 3D freehand ultrasound calibration with real-time accuracy control," MICCAI, vol. 9, 2006, pp. 899-906.

[10] D.M. Muratore, R.L. Galloway Jr. , "Beam calibration without a phantom for creating a 3-D freehand ultrasound system," Ultrasound in Medicine & Biology, 27, 1557–1566.

[11] H. Zhang, F. Banovac, A. White, K. Cleary, "Freehand 3D ultrasound calibration using an electromagnerically tracked needle," Medical Imaging 2006: Visualization, Image-Guided Procedures, and Display, vol. 6141 of Proceedings of SPIE, 775–783, SPIE.

[12] Prager, R W et al. "Automatic Calibration For 3-D Free-Hand Ultrasound." Cambridge University Engineering Department (1997): n. pag

[13] A. Viswanathan, E.M. Boctor, R.H. Taylor, G. Hager , G. Fichtinger , "Immediate ultrasound calibration with three poses and minimal image processing," Proceedings of the 4th International Conference on Medical Image Computing and Computer Assisted Intervention,vol. 3217 of Lecture Notes in Computer Science, 446–454, Springer.

[14] T.K. Chen, A.D.Thurston, M.H. Moghari, R.E Ellis,, P. Abolmaesumi , "A real-time ultrasound calibration system with automatic accuracy control and incorporation of ultrasound section thickness," Progress in Biomedical Optics and Imaging**,** Article number 69182A, 2008.

[15] P.-W. Hsu, R.W.Prager, A.H. Gee, G.M. Treece, "Real-Time Freehand 3D Ultrasound Calibration," Ultrasound Med Biol, pp. 239-251**,** 2008.

[16] R. Kon, J. Leven., K. Kothapalli, E. Boctor, G. Fichtinger, G. Hager, R.H. Taylor, "CIS-UltraCal: An open-source ultrasound calibration toolkit," Progress in Biomedical Optics and Imaging, vol.5750, 2005, pp. 516-523.

[17] B.K.P. Horn, "Closed-form solution of absolute orientation using unit quaternions,"Journal of the Optical Society of America A, vol.4, 1987, pp.629-642.